Article

Electrocatalytic Reactions Mediated by *N*,*N*,*N*‘,*N*‘-Tetraalkyl-1,4-phenylenediamine Redox Liquid Microdroplet-Modified Electrodes: Chemical and Photochemical Reactions In, and At the Surface of, Femtoliter Droplets

Jay D. Wadhawan, Andrew J. Wain, Andrew N. Kirkham, David J. Walton,
Bill Wood, Robert R. France, Steven D. Bull, and Richard G. Compton

J. Am. Chem. Soc., **2003**, 125 (37), 11418-11429• DOI: 10.1021/ja030315p • Publication Date (Web): 23 August 2003

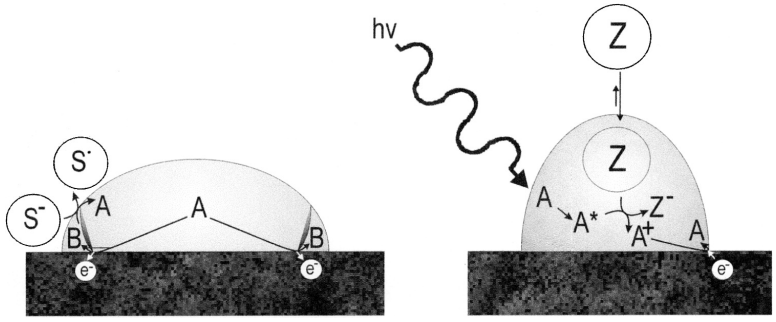

More About This Article

Additional resources and features associated with this article are available within the HTML version:

- Supporting Information
- Links to the 5 articles that cite this article, as of the time of this article download
- Access to high resolution figures
- Links to articles and content related to this article
- Copyright permission to reproduce figures and/or text from this article

View the Full Text HTML

J|A|C|S
ARTICLES
Published on Web 08/23/2003

Electrocatalytic Reactions Mediated by *N*,*N*,*N*′,*N*′-Tetraalkyl-1,4-phenylenediamine Redox Liquid Microdroplet-Modified Electrodes: Chemical and Photochemical Reactions In, and At the Surface of, Femtoliter Droplets

Jay D. Wadhawan,[†] Andrew J. Wain,[†] Andrew N. Kirkham,[‡] David J. Walton,[‡] Bill Wood,[‡] Robert R. France,[§] Steven D. Bull,[||] and Richard G. Compton*,[†]

Contribution from the Physical and Theoretical Chemistry Laboratory, Oxford University, South Parks Road, Oxford OX1 3QZ, United Kingdom; School of Science and the Environment, Coventry University, Priory Street, Coventry CV1 5FB, United Kingdom; Dyson Perrins Laboratory, Oxford University, South Parks Road, Oxford OX1 3QY, United Kingdom; and Department of Chemistry, University of Bath, Claverton Down, Bath BA2 7AY, United Kingdom

Received May 27, 2003; E-mail: richard.compton@chemistry.oxford.ac.uk

Abstract: The electro-oxidation of electrolytically unsupported ensembles of *N*,*N*-diethyl-*N*′,*N*′-dialkyl-*para*-phenylenediamine (DEDRPD, R = *n*-butyl, *n*-hexyl, and *n*-heptyl) redox liquid femtoliter volume droplets immobilized on a basal plane pyrolytic graphite electrode is reported in the presence of aqueous electrolytes. Electron transfer at these redox liquid modified electrodes is initiated at the microdroplet−electrode−electrolyte three-phase boundary. Dependent on both the lipophilicity of the redox oil and that of the aqueous electrolyte, ion uptake into or expulsion from the organic deposits is induced electrolytically. In the case of hydrophobic electrolytes, redox-active ionic liquids are synthesized, which are shown to catalyze the oxidation of L-ascorbic acid over the *surface* of the droplets. In contrast, the photoelectrochemical reduction of the anaesthetic reagent halothane proceeds *within* the droplet deposits and is mediated by the ionic liquid precursor (the DEDRPD oil).

Introduction

The work reported in this paper seeks to interrogate electron transfer processes that take place on the surface of, or within, femtoliter-sized droplets of a water-insoluble redox oil immobilized on a basal plane pyrolytic graphite (bppg) electrode and immersed into an aqueous electrolytic solution. The redox oils employed are *N*-substituted derivatives of 1,4-benzenediamine and are of two categories (see Scheme 1): *N*,*N*,*N*′,*N*′-tetraalkyl-*para*-phenylenediamine (TRPD, R = *n*-butyl, *n*-hexyl, *n*-heptyl, or *n*-nonyl) and *N*,*N*-diethyl-*N*′,*N*′-dialkyl-*para*-phenylenediamine (DEDRPD, R = *n*-butyl, *n*-hexyl, or *n*-heptyl). The electrochemical oxidation of basal plane pyrolytic graphite (bppg) electrodes modified with a random ensemble of microdroplets of TRPD liquids when immersed into aqueous solution was pioneered by Marken.[1−3] The present report now deals with chemical reactions that take place inside or over the immobilized femtoliter volume droplets, building on earlier work[4−16] with nonreactive chemistry. The *unsupported* electroactive liquid microdroplet array is formed via evaporation of a volatile solvent (such as acetonitrile or dichloromethane) from an aliquot of solution exclusively containing the electroactive oil pipeted onto the electrode surface.

Scheme 1. Structure of the *N*,*N*,*N*′,*N*′-Tetraalkyl-*para*-phenylenediamine (TRPD) and *N*,*N*-Diethyl-*N*′,*N*′-dialkyl-*para*-phenylenediamine (DEDRPD) Redox Liquids Employed in This Work

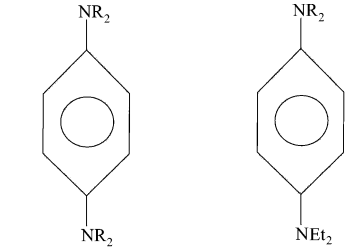

R = *n*-butyl (TBPD), *n*-hexyl (THPD), *n*-heptyl (THePD), *n*-nonyl (TNPD)

R = *n*-butyl (DEDBPD), *n*-hexyl (DEDHPD), *n*-heptyl (DEDHePD)

[†] Physical and Theoretical Chemistry Laboratory, Oxford University.
[‡] Coventry University.
[§] Dyson Perrins Laboratory, Oxford University.
[||] University of Bath.

(1) Marken, F.; Webster, R. D.; Bull, S. D.; Davies, S. G. *J. Electroanal. Chem.* **1997**, *437*, 209.
(2) Marken, F.; Hayman, C. M.; Page, P. C. B. *Electroanalysis* **2002**, *14*, 172.
(3) Marken, F.; Hayman, C. M.; Page, P. C. B. *Electrochem. Commun.* **2002**, *4*, 462.
(4) Marken, F.; Compton, R. G.; Goeting, C. H.; Foord, J. S.; Bull, S. D.; Davies, S. G. *Electroanalysis* **1998**, *10*, 821.
(5) Marken, F.; Blythe, A. N.; Compton, R. G.; Bull, S. D.; Davies, S. D. *Chem. Commun.* **1999**, 1823.
(6) Marken, F.; Blythe, A. N.; Wadhawan, J. D.; Compton, R. G.; Bull, S. D.; Aplin, R. T.; Davies, S. G. *J. Solid State Electrochem.* **2001**, *5*, 170.

10.1021/ja030315p CCC: $25.00

In this work, the mediated oxidation of ascorbate ions using redox-active in situ electrogenerated ionic liquid microdroplet-modified electrodes (where the cationic moiety contains a 1,4-benzenediamine backbone) is first examined, and the kinetics of this liquid−liquid process are estimated; the redox catalytst (the cation radical) is generated at the base of the microdroplets, viz., the electrode−redox oil microdroplet−aqueous electrolyte triple-phase junction, and diffuses and migrates to the surface of the droplets where reaction with ascorbate proceeds. The effect of increasing the length of the *n*-alkyl N-substituents of the redox oil is explored and shown to affect the kinetics of the reaction. Second, the photochemical debromination of halothane by photoexcited TRPD and DEDRPD redox oils is illustrated. In contrast to ascorbate oxidation, reaction of the anaesthetic with the redox oil takes place *within* the organic femtoliter deposits. The results of this work may encourage the deployment of these electrodes as combinatorial sensors or electrolytic reactors. Furthermore, given the use of N-substituted 1,4-benzenediamine compounds as artificial electron donors to both Photosystem I and Photosystem II, and as electron acceptors for Photosystem II,[17] this work may assist in providing in vitro models for photosynthesis.

Experimental Section

Chemical Reagents. All chemical reagents used to prepare aqueous electrolyte solutions were purchased in their purest commercially available forms from Aldrich or British Drug House. Water, with a resistivity of not less than 18 MΩ cm, was taken from an Elgastat filter system (Vivendi, Bucks., UK). Dried and distilled aectonitrile used for the deposition procedure was purchased from Fisons and used without further purification. The *N*,*N*,*N*′,*N*′-tetraalkyl-*para*-phenylenediamine (TRPD, R = *n*-butyl (B), *n*-hexyl (H), *n*-heptyl (He), and *n*-nonyl (N)) redox liquids employed in this work were prepared following a literature procedure;[18] their characteristics have been reported in previous work.[1,11] The synthesis of the *N*,*N*-diethyl-*N*′,*N*′-dialkyl-*para*-phenylenediamine redox liquids (DEDRPD, R = *n*-butyl, *n*-hexyl, *n*-heptyl) followed a similar strategy, using *N*,*N*-diethyl-*para*-phenyelenediamine and the alkyl bromides as the starting materials. The product materials were obtained in pure form after column chromatography with the following spectroscopic characteristics. DEDBPD, elemental analysis: C, 78.34; H, 11.66; N, 9.92. $C_{18}H_{32}N_2$ requires C, 78.26; H, 11.59; N, 10.14. MS (EI) *m*/*z* 276.265; $C_{18}H_{32}N_2$ requires 276. ^{1}H NMR (300 MHz, $CDCl_3$): δ, 6.70 (br s, 4H, Ar-**H**), 3.20 (br m, 8H, $NC\mathbf{H}_2$), 1.50 (br m, 4H, $NCH_2C\mathbf{H}_2$), 1.35 (br m, 4H, $N(CH_2)_2C\mathbf{H}_2$), 1.10 (t, 6H, $NCH_2C\mathbf{H}_3$), 0.90 (t, 6H, $N(CH_2)_3C\mathbf{H}_3$). DEDHPD, elemental analysis: C, 79.53; H, 12.17; N, 8.21. $C_{22}H_{40}N_2$ requires C, 79.52; H, 12.05; N, 8.43. MS (EI) *m*/*z* 332.317; $C_{18}H_{32}N_2$ requires 332. ^{1}H NMR (300 MHz, $CDCl_3$): δ, 6.75 (br q, 4H, Ar-**H**), 3.20 (br m, 8H, $NC\mathbf{H}_2$), 1.55 (br m, 4H, $NCH_2C\mathbf{H}_2$), 1.36 (br m, 12H, $N(CH_2)_2(C\mathbf{H}_2)_3$), 1.12 (t, 6H, $NCH_2C\mathbf{H}_3$), 0.93 (t, 6H, $N(CH_2)_5C\mathbf{H}_3$). DEDHePD, elemental analysis: C, 79.81; H, 12.21; N, 7.59. $C_{24}H_{44}N_2$ requires C, 79.83; H, 12.30; N, 7.77. ^{1}H NMR (300 MHz, $CDCl_3$): δ, 6.70 (br m, 4H, Ar-**H**), 3.15 (br m, 8H, $NC\mathbf{H}_2$), 1.60 (br m, 4H, $NCH_2C\mathbf{H}_2$), 1.30 (br m, 16H, $N(CH_2)_2(C\mathbf{H}_2)_4$), 1.10 (t, 6H, $NCH_2C\mathbf{H}_3$), 0.85 (t, 6H, $N(CH_2)_6C\mathbf{H}_3$). All solutions were degassed with oxygen-free nitrogen (BOC Gases, Guildford, Surrey, UK) prior to experimentation; all experiments were undertaken at 20 ± 2 °C.

Instrumentation. Electrochemical experiments were conducted in a conventional three-electrode cell using a 4.9 mm diameter basal plane pyrolytic graphite working electrode (bppg, Le Carbone, Ltd., Sussex, UK), a platinum wire counter electrode, and a saturated calomel electrode (SCE, Radiometer, Copenhagen, Denmark). As this electrode can be sensitive to high concentrations of perchlorate anions (due to the precipitation of insoluble potassium perchlorate at the calomel frit), this electrode was replaced in some experiments with a sodium-saturated calomel electrode (SSCE). All results reported in this paper are, however, corrected to the SCE. Electrochemical data were recorded using either an Oxford Electrodes analogue potentiostat (Oxford, England) connected to a Lloyd PL3 chart recorder (JJ Instruments, Southampton, UK) or a commercially available computer-controlled potentiostat (Autolab PGSTAT30, Eco Chemie, Utrecht, Netherlands), utilizing a small potential step size.[10] The bppg working electrode was modified with DEDRPD or TRPD redox liquid microdroplets by solvent evaporation of an aliquot of ca. 1 mM redox oil acetonitrile solution. The electrode was cleaned by rinsing with acetonitrile and polishing on silicon carbide paper immediately prior to experimentation.

For photoelectrochemical experiments, a gravity flow system with 3 × 3 mm^2 bppg working electrode located in a rectangular channel cell was employed, as used in previous work.[8] In this experimental configuration, thermal effects due to light absorption are minimized.[8] The channel duct used was 9 cm wide and ca. 1 mm high, with an optically transparent silica cover plate cemented to permit irradiation of the working electrode. A platinum mesh counter electrode was positioned approximately 10 cm downstream of the working electrode, and the SCE reference electrode was placed upstream of the working electrode in a "T"-piece, with the electrode located out of the main solution flow but in electrical contact with the aqueous solution. In this setup, it is was often necessary to shunt the reference and counter electrodes using a 1 nF capacitor, so as to ensure potentiostat stability. Incident light at a selected wavelength was produced from a Wotan XBO 900 W/2 xenon arc lamp used in conjunction with a Jarrell-Ash 82-410 grating monochromator (maximum incident power 2.0 mW cm^{-2}), as used in other work.[19] UV−vis measurements were made by coating an optical grade silica plate (Optiglass Ltd., Hainault, Essex, UK) with the electroactive oil prior to mounting the silica plate into a Unicam UV2 series UV−visible spectrophotometer (Unicam, Cambridge, UK). Spectra due to the radical cation were achieved in a similar manner, after further treatment by dipping the modified silica plate into a 0.1 M aqueous sodium perchlorate solution containing 10 mM potassium ferricyanide.[8]

Results and Discussion

We begin by examining the voltammetry of the three new oils synthesized, of the type *N*,*N*-diethyl-*N*′,*N*′-dialkyl-*para*-phenylenediamine (DEDRPD) (see Scheme 1) via immobilization in the form of microdroplets on a basal plane graphite

(7) (a) Fulian, Q.; Ball, J. C.; Marken, F.; Compton, R. G.; Fisher, A. C. *Electroanalysis* **2000**, *12*, 1012. (b) Ball, J. C.; Marken, F.; Fulian, Q.; Wadhawan, J. D.; Blythe, A. N.; Schröder, U.; Compton, R. G.; Bull, S. D.; Davies, S. G. *Electroanalysis* **2000**, *14*, 1017.
(8) Wadhawan, J. D.; Compton, R. G.; Marken, F.; Bull, S. D.; Davies, S. G. *J. Solid State Electrochem.* **2001**, *5*, 301.
(9) Marken, F.; Compton, R. G.; Goeting, C. H.; Foord, J. S.; Bull, S. D.; Davies, S. G. *J. Solid State Electrochem.* **2001**, *5*, 88.
(10) Schröder, U.; Compton, R. G.; Marken, F.; Bull, S. D.; Davies, S. G.; Gilmour, S. *J. Phys. Chem. B* **2001**, *105*, 1344.
(11) Schröder, U.; Wadhawan, J. D.; Evans, R. G.; Compton, R. G.; Wood, B.; Walton, D. J.; France, R. R.; Marken, F.; Page, P. C. B.; Hayman, C. H. *J. Phys. Chem. B* **2002**, *106*, 8697.
(12) Wadhawan, J. D.; Evans, R. G.; Banks, C. E.; Wilkins, S. J.; France, R. R.; Oldham, N. J.; Fairbanks, A. J.; Wood, B.; Walton, D. J.; Schröder, U.; Compton, R. G. *J. Phys. Chem. B* **2002**, *106*, 9619.
(13) Wadhawan, J. D.; Evans, R. G.; Compton, R. G. *J. Electroanal. Chem.* **2002**, *533*, 71.
(14) Davies, T. J.; Brookes, B. A.; Wilkins, S. J.; Greene, P. R.; Wadhawan, J. D.; Compton, R. G. *J. Phys. Chem. B* **2003**, *107*, 6431.
(15) Wain, A. J.; Lawrence, N. S.; Greene, P. R.; Wadhawan, J. D.; Compton, R. G. *Phys. Chem. Chem. Phys.* **2003**, *5*, 1867.
(16) Wain, A. J.; Wadhawan, J. D.; Compton, R. G. *ChemPhysChem*, in press.
(17) For example, see: Prebble, J. N. *Mitochondria, Chloroplasts and Bacterial Membranes*; Longman: London, 1981; p 317 *f.f.*.
(18) Fuhrop, J.-H.; Bartsch, H. *Liebigs Ann. Chem.* **1983**, 802.
(19) Wadhawan, J. D.; Davies, T. J.; Clegg, A. J.; Lawrence, N. S.; Ball, J. C.; Klymenko, O. V.; Rees, N. V.; Bethell, D.; Woolfall, M. P.; Compton, R. G. *J. Electroanal. Chem.* **2002**, *533*, 33.

(bppg) electrode and immersion into an aqueous solution, and contrast their behavior to the characteristics of the TRPD oils previously reported.[12]

Voltammetry of DEDRPD Microdroplets. A requirement for the voltammetry of microdroplet modified electrodes is that the oil phase is not removed via dissolution on immersion into an aqueous phase. In this work, the tetra-substituted 1,4-benzenediamine backbone is made hydrophobic by using long alkyl chains. The DEDRPD derivatives employed in this work differ from the previously studied liquids in two ways. First, there are two sets of N-substituted alkyl groups on the 1,4-benzenediamine backbone (one being *n*-ethyl), causing a loss in the degree of symmetry of the redox oil molecules. Second, the presence of a smaller length alkyl group ensures the resulting compound is less hydrophobic than the other TRPD oils; *N*,*N*,*N*′,*N*′-tetramethyl-*para*-phenylenediamine (TMPD) is water soluble,[20−29] as is *N*,*N*-diethyl-*para*-phenylenediamine,[30] whereas the TRPD oils used in this work are not measurably soluble in aqueous media.[1−12] Preliminary experiments of all the DEDRPD oils undertaken in 0.1 M sodium perchlorate aqueous solutions at neutral pH (perchlorate is an anion toward the hydrophobic end of the Hofmeister scale[31]) indicated that *N*,*N*-diethyl-*N*′,*N*′-dihexyl-*para*-phenylenediamine (DEDHPD) and *N*,*N*-diethyl-*N*′,*N*′-diheptyl-*para*-phenylenediamine (DEDHePD) are insoluble in water (as seen by no loss of voltammetric signal after immersion in the aqueous solution after 12 h), whereas *N*,*N*-dibutyl-*N*′,*N*′-diethyl-*para*-phenylenediamine (DEDBPD) is *slightly* water soluble, with a small (∼10%) loss of response after immersion for 15 min and a total loss of voltammetric response after 12 h. Consequently, all experiments employing DEDBPD as an electrode modifier were undertaken as soon as possible after immersion into the aqueous electrolyte.

The distribution and size of the microdroplets varies with the amount of material deposited, until a maximum size is obtained as inferred from microscopic studies in previous work.[12,14,15] However, for the *small* quantities (typically <5 nmol redox oil) exclusively employed in this work, the droplets are essentially monodispersed with diameters ca. 4 μm,[12] giving the microdroplets individual volumes of less than ca. 20 fL.

Experiments were next undertaken to study the current−voltage behavior of DEDRPD microdroplets in various aqueous electrolyte solutions. All experiments reported in this paper were carried out at neutral pH; in acidic conditions, N-protonation

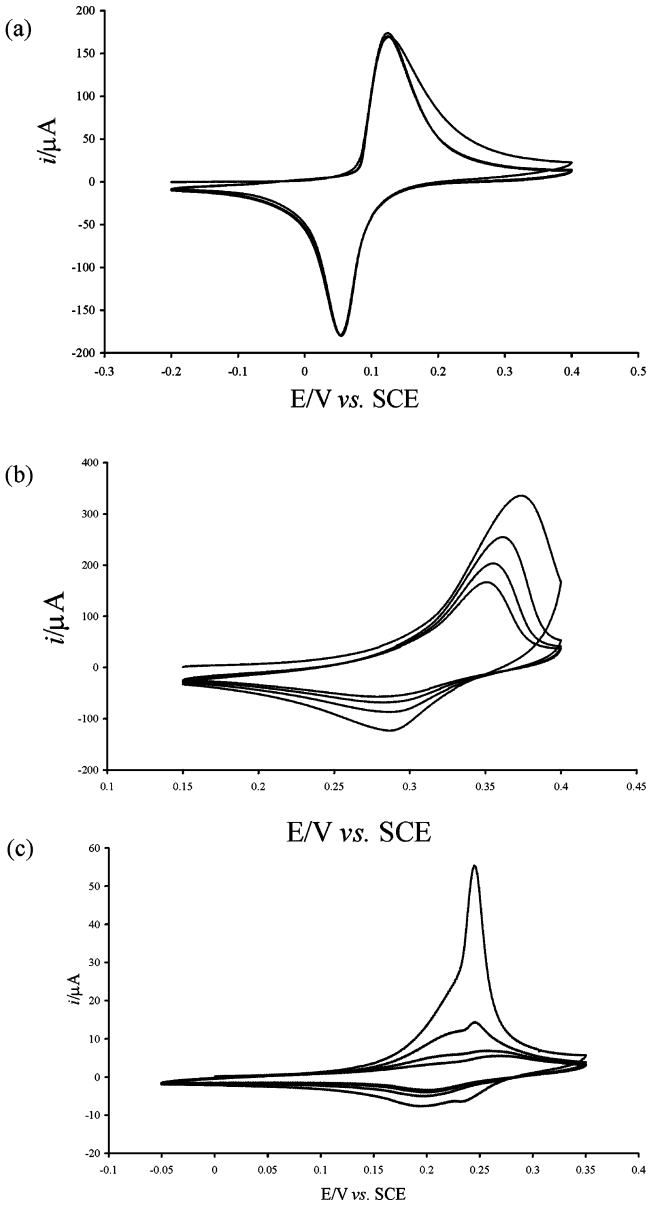

Figure 1. Cyclic voltammograms of DEDRPD microdroplets on a 4.9 mm diameter bppg electrode in the presence of (a) 0.1 M aqueous sodium perchlorate (electrode modified with 5.3 nmol of DEDHePD, scan rate 100 mV s^{-1}, three scans shown); (b) 0.1 M aqueous potassium fluoride (electrode modified with 5.8 nmol of DEDHePD, scan rate 100 mV s^{-1}, four redox cycles are shown); and (c) 0.1 M aqueous potassium nitrate (electrode modified with 5.1 nmol of DEDHPD, scan rate 10 mV s^{-1}, four redox cycles shown).

of the oil occurs,[4,10] in strongly alkaline media, the electrochemically generated cation radical may be attacked by hydroxide ions.[1] Figures 1 and S1−4 (see Supporting Information) illustrate a selection of the typically electrochemically reversible results obtained. Integration of the oxidative voltammetric signal in each case permits the number of electrons discharged at the electrode to be inferred. For 5.4 nmol of the electroactive oil deposited on a 4.9 mm bppg electrode immersed in various electrolytes, the average integrated charge observed to pass during the first oxidation wave was found to be $(3.9 \pm 1.3) \times 10^{-4}$ C, at a scan rate of 10 mV s^{-1}, suggesting the transfer of 0.75 ± 0.25 electrons per redox oil molecule; at the slower scan rate of 2 mV s^{-1}, the average integrated charge was deduced to be $(5.1 \pm 0.1) \times 10^{-4}$ C, implying 0.98 ± 0.02 electrons are

(20) Ravichandran, K.; Baldwin, R. P. *Anal. Chem.* **1983**, *55*, 1586.
(21) For example, see: Lawrence, N. S.; Wadhawan, J. D.; Compton, R. G. *Foundations of Physical Chemistry: Worked Examples*; Oxford University Press: Oxford, 1999; p 140 *f.f.*.
(22) (a) Jacobs, E. E. *Biochem. Biophys. Res. Commun.* **1960**, *3*, 536. (b) Packer, L.; Jacobs, E. E. *Biochim. Biophys. Acta* **1962**, *57*, 373. (c) Utsumi, K.; Packer, L. *Arch. Biochem. Biophys.* **1967**, *122*, 509. (d) Mederos, A.; Domínguez, S.; Hernández-Molina, R.; Sanchiz, J.; Brito, F. *Coord. Chem. Rev.* **1999**, *193*−*195*, 913.
(23) Lee, C. P.; Nordenbrand, K.; Ernster, L. In *Oxidases and Related Redox Systems*; King, T. E., Mason, H. S., Morrison, M., Eds.; Wiley: New York, 1965; Vol. 2, p 960.
(24) Mustafa, M. G.; King, T. E. *Arch. Biochem. Biophys.* **1967**, *122*, 501.
(25) Yu, C. A.; Yu, L.; King, T. E. *J. Biol. Chem.* **1973**, *248*, 528.
(26) Kitani, A.; Miller, L. L. *J. Am. Chem. Soc.* **1981**, *103*, 3595.
(27) Kitani, A.; So, Y.-H.; Miller, L. L. *J. Am. Chem. Soc.* **1981**, *103*, 7636.
(28) Brown, A. P.; Koval, C.; Anson, F. C. *J. Electroanal. Chem.* **1976**, *72*, 379.
(29) (a) Buchanan, R. M.; Calabrese, G. S.; Sobieralski, T. J.; Wrighton, M. S. *J. Electroanal. Chem.* **1983**, *153*, 129. (b) Wildgoose, G. G.; Lawrence, N. S.; Coles, B. A.; Jiang, L.; Jones, T. G. J.; Compton, R. G. *Phys. Chem. Chem. Phys.*, in press.
(30) Lawrence, N. S.; Thompson, M. T.; Davis, J.; Jiang, L.; Jones, T. G. J.; Compton, R. G. *Microchim. Acta* **2001**, *137*, 105.
(31) Hofmeister, F. *Arch. Exp. Pathol. Pharmakol.* **1888**, *24*, 247.

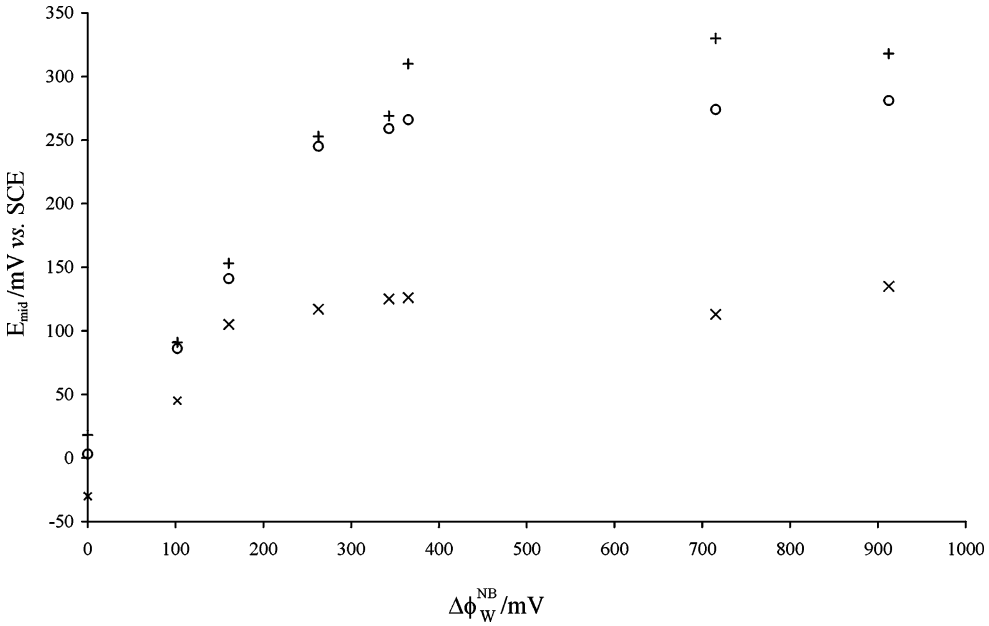

Figure 2. Plots illustrating the dependence of E_{mid} on the anion transfer potential from an aqueous phase to a nitrobenzene phase ($\Delta\phi_W^{NB}$). Key: DEDBPD (×), DEDHPD (○), DEDHePD (+).

discharged per DEDRPD molecule. These data are consistent with the oxidation of the aromatic species to yield the radical cation (i.e., a one-electron oxidation),[1−12] in the "thin layer" limit. Such a limit occurs since electron transfer processes only take place at the junction of all three phases as the DEDRPD microdroplets are electrically nonconducting, preventing the formation of an electrical double layer anywhere else.[1,7,8,10,12,32] This has been demonstrated by the electrocatalytic formation of micrometric silver rings at the *base* of such *para*-phenylenediamine based redox droplets.[12] It should be noted that a second wave is also observed at more positive potentials, due to the formation of the dication;[1,10,11] however, because of the hydrolysis of this species,[21] this redox wave is not considered in this paper.

It is instructive to observe trends in the midpoint potentials ($E_{mid} = {}^1/_2(E_p^{Ox} + E_p^{Red})$) when the nature of both the oil and the supporting electrolyte are varied. These are reported in Table 1 for all N-substituted *para*-phenylenediamine oils considered and for supporting electrolytes with 0.1 M concentration. Two trends are noticeable. First, for a given anion, the midpoint potentials shift to more positive values with increasing total number of carbon units in the alkyl side chains, *viz.*, DEDBPD < TBPD < DEDHPD < DEDHePD < THPD < THePD < TNPD. The second trend in the data in Table 1 is that the midpoint potential shifts to more positive values with increasing anion lipophobicity. This trend is most appreciated via the plots drawn in Figure 2, in which the hydrophobicity of a particular anion is parametrized by its Gibbs energy of transfer across a water−nitrobenzene interface (quoted as the membrane potential). Such plots exhibit a discontinuity, suggesting that two distinct voltammetric pathways exist,[11] *depending on the hydrophobicity of the aqueous-based supporting anion*; lipophilic anions (case (i)) lie on the slopes in Figure 2, whereas, for lipophobic anions (case (ii)), the midpoint potential is independent of the Gibbs transfer energy.[11,13] These categories (case (i) or case (ii) behavior[12]) are explicitly identified in Table 1 and, for a specific anion species, may vary with the oil hydrophobicity (as given by the order noted above). Comparison of Figure 2 with Figures 1 and S1−4 (see Supporting Information) suggests that, for hydrophobic anions (such as perchlorate or hexafluorophosphate), sharp voltammetric signals are observed and these signals are reproduced on repetitive scans (see Figure 1, panel a, and Figures S1 and S2 in the Supporting Information).[1−12] The peak-to-peak potential separation is not zero (as anticipated for a surface confined species), but is typically small, ca. 60−70 mV (Table S1; see Supporting Information), owing to diffusion and migration processes within the organic microdroplets. The very narrow voltammetric responses observed are consistent with reactant−reactant and product−product interactions dominating over reactant−product interactions;[7,33−35] values for the full-width of the voltammo-

Table 1. E_{mid}/mV Data[a] Obtained from Cyclic Voltammograms[b] for the Oxidation of DEDRPD and TRPD Oils[c]

	DEDBPD	TBPD[d]	DEDHPD	DEDHePD	THPD[d]	THePD[d]	TNPD[d]
PF_6^-	−30[i]	−20[i]	3[i]	18[i]	26[i]	41[i]	64[i]
ClO_4^-	45[ii]	63[i]	86[i]	91[i]	109[i]	126[i]	146[i]
SCN^-	105[ii‡]	129[ii]	141[i]	153[i]	178[i]	188[i]	201[i]
Br^-	125[ii]	185[ii]	259[ii‡]	269*	296[i]	318[i]	324[i]
NO_3^-	117[ii‡]	180[ii‡]	245*‡	253*	298[i]	313[i]	327[i]
OCN^-	117[ii‡]	188[ii]	265[ii‡]	290[ii]	365[ii]	381[ii]	385[ii]
Cl^-	126[ii]	193[ii]	266[ii‡]	310[i]	371[ii]	383[ii]	383[i]
SO_4^{2-}	135[ii]	203[ii]	281[ii]	318[ii]	444†	467†	481[ii]
F^-	113[ii]	198[ii]	274[ii]	330[ii]	465†	489†	513[ii]
IO_3^-	134[ii]	238[ii]	268[ii]	336[ii]	470[ii]	481[ii]	501[ii]

[a] All data are reported in mV vs SCE; error ± 5 mV. [b] Oil (5 nmol) was deposited in the form of microdroplets on a 4.9 mm diameter bppg electrode and immersed into 0.1 M aqueous electrolyte. The data were obtained using a san rate of 100 mV s^{-1}. [c] The superscript i or ii identifies the particular oil/anion pair as behaving as either case (i) or case (ii); * indicates that the voltammetric behavior is case (i) at fast scan rates but case (ii) at slow scan rates; † indicates this case is effectively type (ii) behavior, only with very fast kinetics;[12] ‡ indicates those systems that give rise to split waves at slow scan rates. [d] Data taken from refs 11 and 12.

(32) (a) Tasakorn, P.; Chen, J.; Aoki, K. *J. Electroanal. Chem.* **2002**, *533*, 119. (b) Aoki, K.; Tasakorn, P.; Chen, J. *J. Electroanal. Chem.* **2003**, *542*, 51. (c) Rees, N. V.; Klymenko, O. V.; Wadhawan, J. D.; Compton, R. G. *J. Electroanal. Chem.*, in press.

(33) Abruña, H. D. *Coord. Chem. Rev.* **1988**, *86*, 135.

Table 2. Gradients Illustrating the Dependence of E_{mid}, E_p^{Ox}, and E_p^{Red} on the Decadic Logarithm of the Supporting Electrolyte Anion Concentration for 5 nmol of *N*,*N*-Diethyl-*N*′,*N*′-dihexyl-*para*-phenylenediamine (DEDHePD)[a]

	E_{mid}/ mV decade^{-1}	E_p^{Ox}/ mV decade^{-1}	E_p^{Red} /mV decade^{-1}
PF_6^-	−58.7	−94.1	23.2
ClO_4^-	−50.8	−76.5	25.1
SCN^-	−55.5	−76.0	35.1
NO_3^-	−27.9	−49.2	6.7
SO_4^{2-}	11.0	−2.5	19.4
F^-	11.35	−6.2	16.5

[a] The data were obtained using a san rate of 100 mV s^{-1}.

grams at half-maximum are reported in Table S1 (see Supporting Information), which shows that, in agreement with the above interpretation,[33] typical values are less than or equal to the 90.5 mV predicted for thin layer electrochemistry.[33,34] This type of voltammetric behavior is consistent with an "anion insertion" pathway (case (i) type behaviour[12]), viz.,

$$\mathrm{DEDRPD}(l) + \mathrm{X}^-(\mathrm{aq}) - \mathrm{e}^- \rightleftharpoons [\mathrm{DEDRPD}^{+\bullet}\mathrm{X}^-](l) \quad \text{(A)}$$

as electroneutrality within the oil phase has to be maintained during the course of electrolysis and the anion has a low liquid−liquid transfer energy. If the counter anion is poorly coordinating, electrochemical oxidation results in the generation of an ionic liquid. The observed signals are observed to be both electrochemically and chemically reversible,[1−12] and based on process (A), the Nernst equation takes the form:

$$E_{mid} = E_f^\circ + \frac{2.303RT}{F}\log_{10}\left(\frac{[\mathrm{DEDRPD}^{+\bullet}\mathrm{X}^-](l)}{[\mathrm{DEDRPD}](l)}\right) - \frac{2.303RT}{F}\log_{10}([\mathrm{X}^-](\mathrm{aq})) \quad (1)$$

In the above expression, E_f° is the formal potential associated with reaction (A), and as such, it incorporates, among other factors (such as ion pairing energies), a term involving the Gibbs transfer energy of the anion across the aqueous−electroactive oil interface. Given that trends in the latter likely reflect those observed for anion transfer energies across an aqueous−nitrobenzene interface, eq 1 predicts that, all things being equal, a plot of E_{mid} against anion transfer energy expressed as the Galvani potential difference between the aqueous and the nitrobenzene phases should equal one,[11] as observed for the lipophilic anions in Figure 2 (where the gradient of the sloping line is 0.85 ± 0.1). Equation 1 further suggests that DEDRPD oxidation becomes more facile with increasing anion concentration, and that specifically the peak oxidation potential moves to more negative values by ca. 60 mV per decadic increase in supporting electrolyte concentration. Such behavior is observed in these systems, within experimental error (±25 mV decade^{-1}), as indicated in Table 2 for DEDHPD. Errors in the measurement are likely due to ohmic distortions or arise as a result of ion association effects.[12]

For hydrophilic anions (such as fluoride), and for less hydrophilic anions with the more lipophobic oils (viz. DEDBPD, TBPD, and DEDHPD), the independence of the midpoint potential for the oxidation of DEDRPD oils on the Gibbs transfer energy across the aqueous−organic interface suggests that ionic liquid formation in this case is thermodynamically unfavorable.[11,12] The associated voltammetry exhibits waves that decrease in magnitude on successive scans (see Figure 1, panel b, and Figure S3, see Supporting Information), case (ii) behavior, with the peak potentials on successive waves in some cases moving to slightly more negative potentials, possibly as a result of the aqueous electrolyte partitioning into the organic deposits[13] or due to the smaller size of the microdroplets causing less ohmic drop. Integration of the first oxidative wave still reveals the transfer of a single electron per DEDRPD molecule, suggesting that the radical cation dissolves out of the organic microdroplets during oxidation:[11−13]

$$\mathrm{DEDRPD}(l) - \mathrm{e}^- \rightleftharpoons \mathrm{DEDRPD}^{+\bullet}(\mathrm{aq}) \quad \text{(B)}$$

The increasingly diminishing current occurs as the cation radical diffuses out of the diffusion layer, causing less available material to redeposit on the electrode surface in the reverse sweep.[11−13] It has been shown in previous work for the TRPD oils that although electron transfer is initiated at the three-phase junction, the product diffuses out from over the whole microdroplet, and with two-thirds order kinetics.[12] In this model, the voltammograms are treated simplistically as thin layer responses with no diffusional contribution, giving rise to the equation:[12,13]

$$\sqrt{Q^{1/3}} = \sqrt{Q_0^{1/3}} - \frac{k_{eff}\sqrt{F^{1/3}}}{3}t \quad (2)$$

in which F is the Faraday constant, Q_0 is the charge required to oxidize all the immobilized oil into the cation radical on the first oxidative scan, and k_{eff} is an effective two-thirds order rate constant. Plots of the cube root of the observed oxidative charge against time were linear in agreement with dissolution from the microdroplet liquid−liquid interface for DEDHePD oxidation in the presence of NO_3^-, OCN^-, Br^-, F^-, and SO_4^{2-} anions; the k_{eff} values deduced from the gradient of the plots are reported in Table S2 (see Supporting Information). The average k_{eff} observed is 1.1×10^{-5} mol$^{1/3}$ s^{-1}, in good agreement with the 9.6×10^{-6} mol$^{1/3}$ s^{-1} predicted by eq 16 of ref 12 (using an average number of carbon atoms in the alkyl chains (N_C) as $^1/_4(2 \times 2 + 7 \times 2) = 4.5$):

$$k_{eff}^{av} = 2.25 \times 10^{-5} - 8.6 \times 10^{-6}\ln(N_C);\ R^2 = 0.96 \quad (3)$$

Thus, as with the TRPD oils, dissolution takes place from the liquid−liquid interface. The breakdown of the model for the other, more hydrophilic oils is likely due to other factors operating (vide infra).[13]

As an aside, we note that the Gibbs energy for the transfer of the radical cation to the water phase may be estimated from the intersection of the two lines in Figure 2 (assuming nitrobenzene sufficiently mimics the electroactive oil) to be −17 kJ mol^{-1} (DEDBPD), −27 kJ mol^{-1} (DEDHPD), and −44 kJ mol^{-1} (DEDHePD), in agreement with the hydrophobicity order inferred earlier.

(34) Broad, A. M. *Bondening Electrochemical Horizons*; Oxford University Press: Oxford, 2002.
(35) (a) Park, S. G.; Aoki, K.; Tokuda, K.; Matsuda, H. *J. Electroanal. Chem.* **1985**, *195*, 157. (b) Matsuda, H.; Aoki, K.; Tokuda, K. *J. Electroanal. Chem.* **1987**, *217*, 15. (c) Lee, C.-W.; Bard, A. J. *J. Electroanal. Chem.* **1988**, *239*, 441. (d) Richardson, T.; Roberts, G. G.; Barghout, R.; Compton, R. G.; Riley, D. J. *Electroanalysis* **1991**, *3*, 757.

Process (B) suggests that the microdroplet dissolution process is independent of the anion; that is, varying the concentration of the hydrophilic anion in the aqueous phase will not cause the oxidation potential to shift. However, experiments conducted with a varying concentration of aqueous electrolyte in the range 0.01−1.0 M (see Table 2) indicate that, within experimental error, the midpoint potential and both the peak oxidation and reduction potentials are independent of the anion concentration only for "hard" anions such as fluoride, sulfate, and those for which the voltammetric signals are narrow (see Table S1 in the Supporting Information); other "soft" anions, such as nitrate and bromide, cause the voltammetric waves to be broad (*q.v.* Table S1 in the Supporting Information), and as illustrated in Table 2, the peak oxidation potential shifts by almost 60 ± 10 mV per decadic change in the anion concentration. In addition, the potential of the reverse peak is observed to be, within experimental error, effectively *independent of the aqueous supporting electrolyte concentration*. Hence,[13] in this latter case, an electrochemically induced anion-facilitated cation dissolution process may occur, in which aqueous based ions adsorb on the surface of the DEDRPD and TRPD microdroplets, enabling the formation of a transient tight ion pair upon electrochemical oxidation of the microdroplets, and as which the cation is expelled (and in so doing preserving the electrostatically neutral environment of the microdroplet), giving rise to the 60 mV dependence of the oxidation peak potential on anion concentration.[13] The fact that the reverse potential is independent of the concentration of the anion implies that, in the aqueous phase, the tight cation/anion pair breaks down in the aqueous phase, and, on the reverse sweep, the back reaction of process (B) takes place, with a reduced amount of material redeposited owing to the loss of the aqueous cation radical from the Nernst layer.[13] There are thus two pathways for electrochemically induced cation dissolution.

The electrochemistry of the homologous oils in the presence of nitrate-based electrolytes provides an interesting admixture of all the cases described above (see Figure 1c and Figure S4 in the Supporting Information), as the transfer energy of nitrate from the aqueous phase into nitrobenzene lies in the "insertion" regime or in the "dissolution" regime, depending on the hydrophobicity of the redox liquid. In the presence of the higher homologues (DEDHePD, THPD, THePD, and TNPD), oxidation to the radical cation (at fast scan rates) induces nitrate insertion at the three-phase junction, as evidenced by the narrow, stable voltammetric signals in Figure S4(i) (see Supporting Information).[11,12] In contrast, as with the voltammetry of microdroplets of all other N-substituted *para*-phenylenediamine derivatives (viz. DEDHPD, TBPD, and DEDBPD), when the voltage sweep rate slows down, oxidation causes the cation radical to diffuse out of the oil phase (see Figure 1c and Figure S4(ii) in the Supporting Information). In Figure 1c, the dissolution waves not only are broad (see Table S1 in the Supporting Information) but also exhibit *split signals*, which become increasingly more pronounced as the experimental time scale increases. Such split spignals are also observed for the voltammetry of DEDHPD and DEDBPD in the presence of aqueous OCN^-, Cl^-, and Br^- ions. The presence of split waves has been observed previously for the case of solid microparticles of *N*,*N*′-diphenyl-*para*-phenylenediamine abrasively immobilized on an electrode[36] and for microdroplets of *n*-butylferrocene deposited on a graphite electrode surface[13] and rationalized as due to surface versus bulk electrochemistry in the former case[36] and adsorption of the neutral parent in the latter.[13] The sharper second signal observed in this work (see Figure 1c) corresponds to a reversible adsorbed redox couple.

The remainder of this paper is devoted to the induction of electron-transfer processes across the liquid−liquid interface via redox catalysis. Würster's Blue ($TMPD^{+\bullet}$) is known to mediate the *homogeneous* solution oxidation of biological redox compounds,[20,22,23] with particular emphasis on the mediated oxidation of vitamin C (L-ascorbic acid),[22] NADH,[24] and various ferrocyctochromes.[25] It is appreciated that the ability to control the amount of Würster's Blue present may permit the sensing of the biological analyte at a potential more negative than that required for the oxidation of the latter. Hence, work by Miller and co-workers[26,27] illustrated the electrocatalytic recognition of both ascorbate and NADH via homogeneous aqueous phase oxidation of TMPD, with the former compound being oxidized by Würster's Blue and NADH being oxidized by the dication,[26] $TMPD^{2+}$; Baldwin and Ravichandran demonstrated the electroanalysis of ascorbate and NADH via a TMPD-modifed carbon paste electrode,[20] and owing to the inability to adsorb TMPD on an electrode,[28] Wrighton et al.[29a] used electrodes chemically modified with a silianised derivative of TMPD to effect the catalytic oxidation of both ascorbate and ferrocytochrome *c* via the *intra muros* electrochemical generation of the immobilized N-substituted *para*-phenylenediamine cation radical. Thus, we first consider the reaction between the electrogenerated ionic liquid microdroplets and L-ascorbate.

Electrocatalytic Reaction at the Electrode−Oil−Electrolyte Triple-Phase Junction. The oxidation of 5 mM ascorbic acid on a freshly cleaved bppg electrode revealed an oxidation peak at 0.17 V versus SCE when the electrode was immersed into a 0.1 M aqueous phosphate buffer solution at pH 7 in agreement with the results reported by Baldwin and Ravichandran.[20] To ensure redox catalysis takes place at the liquid−liquid interface, rather than at the exposed, nonblocked parts of the bppg electrode, or even within the microdroplets, all subsequent experiments employing a redox liquid microdroplet-modified electrode were undertaken using a supporting electrolyte containing an hydrophobic anion (ClO_4^- or PF_6^-); as can be seen from Table 1, the midpoint potential for all TRPD and DEDRPD oil oxidations in the presence of aqueous electrolytes containing either of these anions in 0.1 M concentration occurs at potentials *less* than 0.15 V versus SCE, and thus the immobilized oil microdroplets are more easily oxidized than ascorbate. Further, owing to the greater hydrophobicity of these anions compared with ascorbate,[37] the former ions likely preferentially insert into the redox oil microdroplets, forming an ionic liquid with which ascorbate reacts.

Figure 3a illustrates the voltammetry of a bppg electrode modified with 5.4 nmol THPD and immersed into an aqueous 0.1 M sodium perchlorate solution containing 50 mM ascorbic acid at pH 7.0, at a voltage sweep rate of 10 mV s^{-1}. At this pH value, ascorbic acid exists in its deprotonated form.[38] The presence of ascorbate ions has a dramatic effect on the voltammetry. First, during the oxidative scan, more charge is passed

(36) Lawrence, N. S.; Jiang, L.; Jones, T. G. J.; Compton, R. G. *Anal. Chem.* **2003**, *75*, 2054.
(37) Kocherginskii, N. M.; Sakste, N. I.; Berkovich, M. A.; Devichenskii, V. M. *Biofizika* **1981**, *26*, 442.

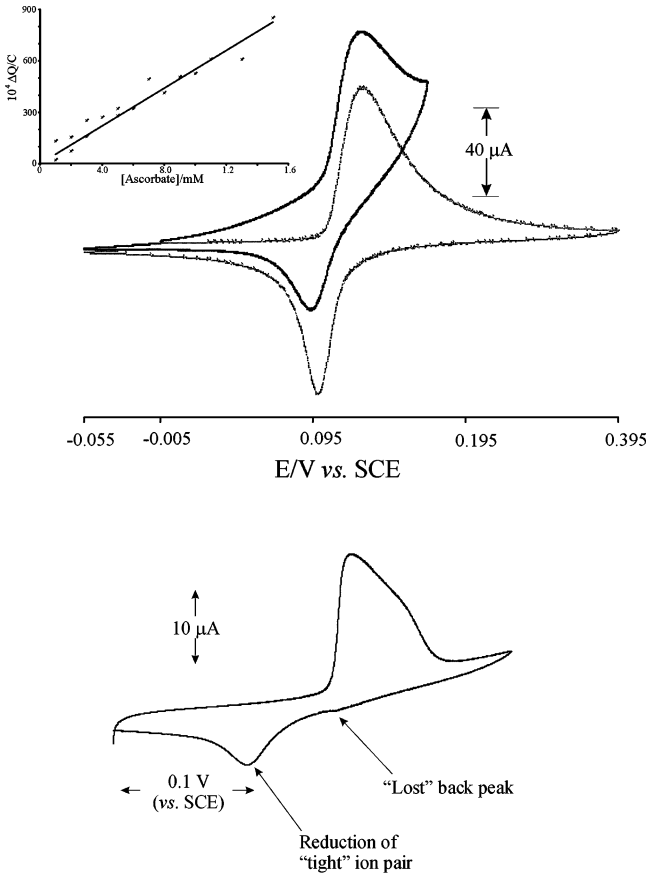

Figure 3. (a) Cyclic voltammograms (scan rate 10 mV s^{-1}) illustrating the electrocatalytic oxidation of ascorbate; 5.4 nmol of THPD deposited on the surface of a 4.9 mm diameter bppg electrode immersed into aqueous 0.1 M sodium perchlorate solution, in the presence (solid line) and absence (dotted line) of 50 mM ascorbic acid at pH 7. The insert illustrates the charge difference inferred from cyclic voltammogram (scan rate 5 mV s^{-1}) variation with ascorbic acid concentration for the oxidation of 5.4 nmol of THPD immobilized as microdroplets on a 4.9 mm diameter bppg electrode immersed in 0.1 M potassium hexafluorophosphate containing 0.1 M phosphate buffer solution at pH 7. (b) Cyclic voltammogram (scan rate 5 mV s^{-1}) of 6.0 nmol of TBPD immobilized on a 4.9 mm diameter bppg electrode immersed into an aqueous 0.1 M phosphate buffer solution at pH 7 containing 0.1 M potassium hexaflurophosphate and 1 mM ascorbic acid. The starting potential was −0.2 V vs SCE. The "lost" pack peak observed (see text) contrasts with that observed in the absence of ascorbate (*q.v.* Figure 7b(i) of ref 12).

compared to the case when ascorbic acid is not present, as inferred from the bigger voltammetric signal (see Figure 3a). Second, on the reverse scan, the magnitude of the back peak is considerably diminished in the presence of ascorbate ions. These observations suggest redox catalysis occurs at the liquid−liquid interface;[39] insertion of ascorbate ions (AH^-) does not take place since they are less hydrophobic compared to PF_6^- ions and the ascorbate products of the oxidation are sufficiently hydrophilic not to transfer.[39] The greater current and amount of charge passed compared to the THPD(*l*) → $THPD^{\bullet+}$(*l*) conversion suggests mediated oxidation of ascorbate (see Scheme 2); the reduced back peak indicates that $THPD^{\bullet+}$ electrochemically generated at the triple-phase boundary is reduced by ascorbate

Scheme 2. Schematic Diagram Illustrating the Electrocatalysis of L-Ascorbate by $THPD^{+\bullet}ClO_4^-$ [a]

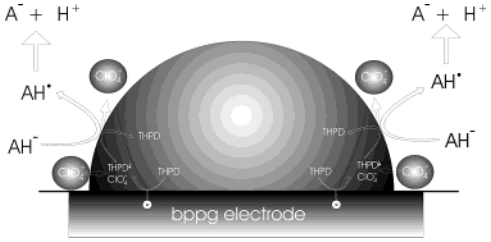

[a] For simplicity, only one microdroplet is considered.

(process (C)) at a rate competitive with its reduction at the three-phase boundary (process (D)):

$$[THPD^{\bullet+}PF_6^-](l) + AH^-(aq) \xrightarrow{k_{cat}} THPD(l) + AH^{\bullet}(aq) + PF_6^-(aq) \quad (C)$$

$$[THPD^{\bullet+}PF_6^-](l) + e^- \rightleftharpoons THPD(l) + PF_6^-(aq) \quad (D)$$

The "outer sphere" catalytic oxidation of ascorbate ions (reaction (C)) is essentially irreversible, since the kinetics of the electron transfer from TMPD to ascorbate are fast, and the back electron transfer is slow; in aqueous solutions at pH 7, Prieto and co-workers[40] demonstrated that proton loss from the radical generated after electron transfer from ascorbate to an electrode creates a degree of *irreversibility* in the ECE oxidation scheme:

$$AH^- - e^- \rightarrow AH^{\bullet}$$

$$AH^{\bullet} \rightarrow A^{\bullet-} + H^+$$

$$A^{\bullet-} - e^- \rightarrow A$$

It is not clear where the oxidation of $A^{\bullet-}$ occurs; this is probably at the surface of the droplets but may also be at the exposed carbon electrode surface. The above behavior is not limited to the tetra-hexyl derivative; analogous behavior was observed for *all* TRPD and DEDRPD systems studied. A particularly noteworthy result is that of $TBPD^{+\bullet}$ reaction with ascorbate, where the back peak thought to arise from reduction of loosely ion paired $TBPD^{+\bullet}$ is almost completely lost, whereas that thought to be due to the tight ion pair[12] remains unaffected (see Figure 3b).

Deducing the kinetics of the liquid−liquid electron transfer process is complicated by a variety of *possible* processes, such as diffusion of ascorbate within the aqueous phase, diffusion and migration of the $THPD^{\bullet+}$ radical cation within the microdroplets, or even diffusion of ascorbate into and within the THPD microdroplets. It is reasonable to hypothesize that ascorbate ions do not penetrate the THPD microdroplets, since they are in ionic form in the aqueous solution, while THPD is a molecular oil, and it was observed that ascorbic acid crystals are insoluble in THPD. Further, the more hydrophobic supporting electrolyte anion likely inserts and remains in the resulting ionic liquid as inferred by the oxidation peak at 0.13 V versus SCE in Figure 3a (*q.v.* Table 1). Thus, we propose that the mediated electrocatalysis results from electron transfer across the liquid−liquid interface.[39] As the $THPD^{+\bullet}$ cation radical is electrochemically generated at the triple-phase boundary, het-

(38) L-Ascorbic acid has *two* pK_a values, which, at 298 K, are $pK_{a1} = 4.17$ and $pK_{a2} = 11.57$; see: Dryhurst, G.; Kadish, K.; Scheller, F.; Reneberg, R. *Biological Electrochemistry*; Academic Press: New York, 1982; Vol. 1, p. 256.

(39) Suzuki, M.; Umetani, S.; Matsui, M.; Kihara, S. *J. Electroanal. Chem.* **1997**, *420*, 119.

(40) Prieto, F.; Coles, B. A.; Compton, R. G. *J. Phys. Chem. B* **1998**, *102*, 7442.

Scheme 3. Schematic Illustration of the Droplet Sizes Used in the Model (See Text)

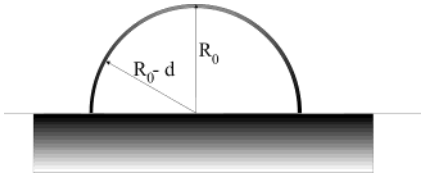

erogeneous electron transfer to ascorbate may take place at this site or, if diffusion of the cation radical within the microdroplets is fast, over the surface of the droplets. To circumvent this problem, we consider the electron transfer process in a "thin layer" regime. We further assume that the rate of the nonmediated heterogeneous electron transfer to ascorbate at the naked parts of the partially blocked microdroplet-modified electrode is slow, so that electron transfer from ascorbate to $THPD^{\bullet+}$ at the aqueous−microdroplet interface dominates,[29a] although the former plays an increasingly more significant role with the more hydrophobic oils (*q.v.* Table 1) and at smaller electrode surface coverage with microdroplets. (Partially blocked electrodes have been shown[14,41] to yield apparent heterogeneous electron transfer rates smaller than those at nonblocked electrodes of the same geometric area.) We assume that the microdroplet-modified electrode consists of a monodispersed set of N femtoliter droplets, each of radius R_0. If the electrode is modified with N_0 moles of THPD, we may write

$$N_0 = n_0 N \tag{4}$$

where n_0 is the number of THPD moles in a *single* microdroplet. As the redox liquid modified electrode operates under "thin layer" conditions (viz. in the limit of slow scan rate, so full droplet conversion occurs), the number of moles of $THPD^{+\bullet}$ electrochemically generated is N_0 (i.e., n_0 moles of $THPD^{+\bullet}$ radical cations are present in each microdroplet). If the reaction between $THPD^{+\bullet}$ and ascorbate occurs at the liquid−liquid interface (see Scheme 3), the rate of reaction per single microdroplet is given by the second order equation:

$$\text{Rate} = k_{cat} n_{shell} [AH^-]_{bulk} \tag{5}$$

in which the units for the reaction rate are moles of $THPD^{+\bullet}$ per second, k_{cat} is the rate constant for the liquid−liquid electron transfer process (units $M^{-1}\ s^{-1}$), $[AH^-]_{bulk}$ is the bulk solution concentration of ascorbate ions, and n_{shell} is the number of $THPD^{+\bullet}$ ions lying in a shell of thickness d (the spherical thickness of a single $THPD^{+\bullet}$ ion), given by the expression:

$$n_{shell} = \frac{n_0}{\frac{2}{3}\pi R_0^3} \times \frac{2}{3}\pi(R_0^3 - (R_0 - d)^3) \approx \frac{3 n_0 d}{R_0} \tag{6}$$

Hence, the total reaction rate can be estimated using eqs 4−6:

$$\text{Rate} = \frac{3d}{R_0} k_{cat} N_0 [AH^-]_{bulk} \tag{7}$$

Experimentally, as inferred from the voltammograms, a measure of the degree of electrocatalysis (and thus of the electron transfer across the liquid−liquid interface) is the increase in the charge passed in the presence *cf.* absence of ascorbate, ΔQ_{obs}. Hence, assuming that $A^{\bullet-}$ reacts rapidly at the droplet surface with $THPD^{+\bullet}$, the number of moles of THPD formed as a result of electron transfer across the liquid−liquid phase boundary is $\Delta Q_{obs}/2F$. Estimation of the kinetics of the electron transfer process requires knowledge of the time for which electron transfer is possible, which effectively is at any time after $THPD^{+\bullet}$ has been generated at the electrode−microdroplet−aqueous electrolyte triple-phase boundary. Thus, electron transfer across the microdroplet−aqueous phase boundary is possible within a time, τ, given by

$$\tau = \frac{\Delta E}{\upsilon} \tag{8}$$

where υ is the potential scan rate during the electrochemical oxidation and ΔE is the difference between the starting and finishing potentials of the sweep. Thus, a lower limit on the rate of formation of THPD by electron transfer across the liquid−liquid interface can be estimated from

$$\text{Rate} \approx \frac{\Delta Q_{obs}}{2F\tau} \tag{9}$$

Comparison of eq 9 with eq 7 yields

$$\Delta Q_{obs} = \frac{6d}{R_0} k_{cat} F \tau N_0 [AH^-]_{bulk} \tag{10}$$

The above neglects the rate of diffusion of ascorbate ions within the aqueous solution. It has been shown that, in some cases, electrocatalysis at chemically modified electrodes is limited by diffusion within the aqueous phase.[42] If diffusion in the aqueous phase were to be significant, the limiting diffusional rate of ascorbate to the liquid−liquid interface (of area equal to that of the whole electrode, A) would be

$$\text{Rate} = \frac{DA[AH^-]_{bulk}}{\delta} \tag{11}$$

In the above equation, D is the diffusion coefficient of ascorbate anions in aqueous media, and δ is in the order of the droplet size or if all the droplets overlap, then δ is the Nernst layer thickness of the size 100−200 μm, in unstirred aqueous solutions. The steady-state reaction rate equals the diffusion rate, and thus,

$$\delta = \frac{2DAF\tau[AH^-]_{bulk}}{\Delta Q_{obs}} \tag{12}$$

For typical experimental values ($D = 10^{-5}\ cm^2\ s^{-1}$, $A = 0.2\ cm^2$, $\tau = 30$ s, $[AH^-]_{bulk} = 1$ mM, and $\Delta Q_{obs} = 10^{-4}$ C), δ (~1 mm) is much larger than the diameter of the microdroplets (~4 μm[12]), suggesting that diffusion in the aqueous phase is

(41) Amatore, C. A.; Savéant, J.-M.; Tessier, D. *J. Electroanal. Chem.* **1983**, *147*, 39.

(42) (a) Murray, R. W. *Philos. Trans. R. Soc. London, Ser. A* **1981**, *302*, 253. (b) Murray, R. W. *Acc. Chem. Res.* **1980**, *13*, 135. (c) Murray, R. W. In *Electroanalytical Chemistry*; Bard, A. J., Ed.; Marcel Dekker: New York, 1984; Vol. 13, p 191. (d) Murray, R. W.; Ewing, A. G.; Durst, R. A. *Anal. Chem.* **1987**, *59*, 379A; (e) Wring, S. A.; Hart, J. P. *Analyst* **1992**, *117*, 1215. (f) Gorton, L.; Domínguez, E. *Rev. Mol. Biotechnol.* **2002**, *82*, 371. (g) Albery, W. J.; Hillman, A. R. *J. Electroanal. Chem.* **1984**, *170*, 27. (h) Andrieux, C. P.; Savéant, J.-M. In *Molecular Design of Electrode Surfaces*; Murray, R. W., Ed.; Wiley: New York, 1992; p 207.

Table 3. Reaction-on-a-Drop Analysis (Eq 10) of the Reaction between DEDRPD and TRPD Radical Cations and L-Ascorbate[a]

	gradient of plot /C M^{-1}	$6dk_{cat}/R_0$ /M^{-1} s^{-1}	k_{cat} [b] /M^{-1} s^{-1}
DEDBPD[c]	0.2373 ± 0.012	10.9 ± 0.5	7237 ± 366
DEDHPD[d]	0.1298 ± 0.012	5.8 ± 0.5	3876 ± 358
TBPD[e]	0.0798 ± 0.012	2.3 ± 0.3	1257 ± 230
THPD[f]	0.0553 ± 0.012	3.2 ± 0.7	2139 ± 464
DEDHePD[g]	0.0289 ± 0.012	1.3 ± 0.5	866 ± 360
THePD[h]	0.0245 ± 0.012	1.8 ± 0.9	1184 ± 580
TNPD[i]	0.0232 ± 0.012	3.0 ± 1.6	2005 ± 1039

[a] Data obtained from cyclic voltammograms recorded at a scan rate of 5 mV s^{-1}, in 0.1 M phosphate buffer solution containing 0.1 M potassium hexafluorophosphate, using a modified 4.9 mm diameter bppg electrode. [b] Assuming $d = 5$ Å and $R_0 = 2$ μm. [c] Electrode modified with 5.7 nmol of DEDBPD, $\tau = 40$ s. [d] Electrode modified with 5.8 nmol of DEDHPD, $\tau = 40$ s. [e] Electrode modified with 6.0 nmol of TBPD, $\tau = 60$ s. [f] Electrode modified with 6.0 nmol of THPD, $\tau = 30$ s. [g] Electrode modified with 5.8 nmol of DEDHePD, $\tau = 40$ s. [h] Electrode modified with 6.0 nmol of THePD, $\tau = 24$ s. [i] Electrode modified with 5.7 nmol of TNPD, $\tau = 14$ s.

not significant and that the rate of electron transfer across the liquid−liquid interface limits the reaction.

Equation 10 suggests that the difference in charge between the mediated and non-catalyzed cases is directly proportional to the concentration of ascorbate in the aqueous phase. Plots of ΔQ_{obs} against ascorbate concentration were found to exhibit this predicted behavior (see the inset of Figure 3a), permitting the estimation of $(6d/R_0)k_{cat}$ from the gradient of such plots. Table 3 reports the results of these analyses for all seven oils studied, together with estimates of k_{cat} for the case of $d = 5$ Å and $R_0 = 2$ μm. It can be seen that the reactivity generally increases with decreasing total substitution length, viz. in the order DEDBPD > DEDHPD > TBPD = THPD > DEDHePD = THePD = TNPD. We attribute this order to the greater number of cations per unit surface area for the lower homologues. Wrighton and co-workers[29a] deduced the electrocatalytic kinetics of the reaction between a chemically immobilized *N*,*N*,-dimethyl-*N*′-ethyl-*N*′-(trimethoxysilyl-4-butyl)-1,4-benzenediamine cation radical with ascorbate to be ca. 100 M^{-1} s^{-1}, compared with the aqueous homogeneous oxidation of ascorbate by Würster's Blue to be approximately 800 M^{-1} s^{-1},[29a] in agreement with the recent results by Lawrence and co-workers (at 298 K).[29b] These data exhibit similar trends to those described above.

We next turn to examine the possibility of photoelectrochemical redox catalysis at TRPD microdroplets. Photochemically induced reactions may take place at faster rates owing to activation of the reaction, and the possibility of a subsequent light-induced bond cleavage may cause the electron transfer reaction to be irreversible.[43]

Photochemically Induced Electrocatalytic Processes. It has been shown that TRPD redox liquids absorb UV light maximally at around 300 nm,[8,10] as a result of a $\pi-\pi^*$ transition,[44] and the corresponding cation radicals absorb light in both the UV and visible ranges at around 300 and 550 nm, respectively.[8,10] Table S3 (see Supporting Information) reports the absorption peaks of all the TRPD and DEDRPD redox oils and their corresponding cation radicals when immobilized on a silica plate.

In the presence of light (chopped with ca. 20−50 s intervals, ca. 2 mW cm^{-2}, 280 nm, 0.1 M $NaClO_4$, solution flow rate 0.003 cm^3 s^{-1}, a flow rate sufficiently slow to not cause voltammetrc distortions[8]), significant photocurrent responses were detected for both photooxidation at an applied potential of 0.4 V versus SCE, a voltage at which the ionic liquid is electrochemically generated ($THPD^{\bullet+}ClO_4^-$), and photoreduction at 0.0 V versus SCE (where the neutral precursor molecule exists).[8] Photocurrents were not observed at naked bppg electrodes.[8] In Figure 4a, both photochemical responses are illustrated and can be seen to reach a steady-state limit, albeit with different sizes, but both photocurrents being in the order of a few nanoamps for 5 nmol of THPD on the bppg surface. Previous work[8] suggests the *tiny* reductive photocurrents observed when the electrode is potentiostated at 0 V versus SCE are due to electron transfer to oxygen dissolved in the microdroplets (the electrode is prepared on the "open bench"). As this process can take place anywhere within the microdroplets, the time lag that is observed is due to positive charge migration (possibly via electron hopping) to the three-phase boundary, at which it is reduced, giving rise to the "photocurrent". The photocurrents observed at wavelengths less than 400 nm and around 550−600 nm when the microdroplet-modified electrode consists of the ionic liquid $THPD^{+\bullet}ClO_4^-$ are thought to arise from the disproportionation of the excited radical cation.[8] In both cases, light absorption may take place anywhere within the microdroplets; in contrast, electron transfer may only take place at the three-phase boundary. Hence, steady-state photocurrents are not observed immediately in either case, as a result of positive charge propagation (possibly via hole hopping) within the microdroplets to the triple-phase junction, at which it is reduced.

When halothane (2-bromo-2-chloro-1,1,1-trifluoroethane) is present in the aqueous phase, and the electrode potentiostated at 0 V versus SCE (a potential at which halothane is electrochemically inert), large reductive photocurrents were again observed on illumination at wavelengths < 400 nm (see Figure 4b). These photocurrents (typically ca. 70 nA for 5.4 nmol of THPD immoblised at 290 nm, when 10 mM halothane is present in aqueous solution) diminished in size on increasing the electrode potential (not shown), suggesting that the photocurrents arise as a consequence of a charge transfer reaction occurring between THPD and halothane; the photocurrents are *much* greater than in the THPD-only case, and the direct, nonmediated photoelectrochemical reduction of halothane was ruled out owing to the large negative potential required for halothane reduction in aqueous solutions.[45] Charge transfer between photoexcited THPD and halothane is likely, given the earlier work using TMPD as an electron donor to haloalkanes species.[22d,46−48] The mediated electron transfer process is irreversible owing to bromide displacement from the resulting anion radical:[45]

(43) (a) Moutet, J.-C.; Reverdy, G. *J. Chem. Soc., Chem. Commun.* **1982**, 654. (b) Moutet, J.-C.; Reverdy, G. *Nouv. J. Chim.* **1983**, *7*, 105.
(44) Cadogan, K. D.; Albrecht, A. C. *J. Phys. Chem.* **1969**, *73*, 1868.
(45) (a) Albery, W. J.; Hahn, C. E. W.; Brooks, W. N. *Br. J. Anaesth.* **1981**, *53*, 447. (b) Mount, A. R.; Appleton, M. S.; Albery, W. J.; Clark, D.; Hahn, C. E. W. *J. Electroanal. Chem.* **1992**, *334*, 115. (c) Mount, A. R.; Appleton, M. S.; Albery, W. J.; Clark, D.; Hahn, C. E. W. *J. Electroanal. Chem.* **1992**, *340*, 287. (d) Hahn, C. E. W. *Analyst* **1998**, *123*, 57R.
(46) (a) Meyer, W. C. *J. Phys. Chem.* **1970**, *74*, 2118. (b) Meyer, W. C. *J. Phys. Chem.* **1970**, *74*, 2122. (c) Meyer, W. C. *J. Phys. Chem.* **1970**, *74*, 2127.
(47) (a) Cohen, S. G.; Parola, A.; Parsons, G. H., Jr. *Chem. Rev.* **1973**, *73*, 141. (b) Fitzgerald, E. A., Jr.; Wuelfing, P., Jr.; Richtol, H. H. *J. Phys. Chem.* **1971**, *75*, 2737.
(48) Eberson, L.; Ekström, M. *Acta Chem. Scand.* **1989**, *43*, 86.

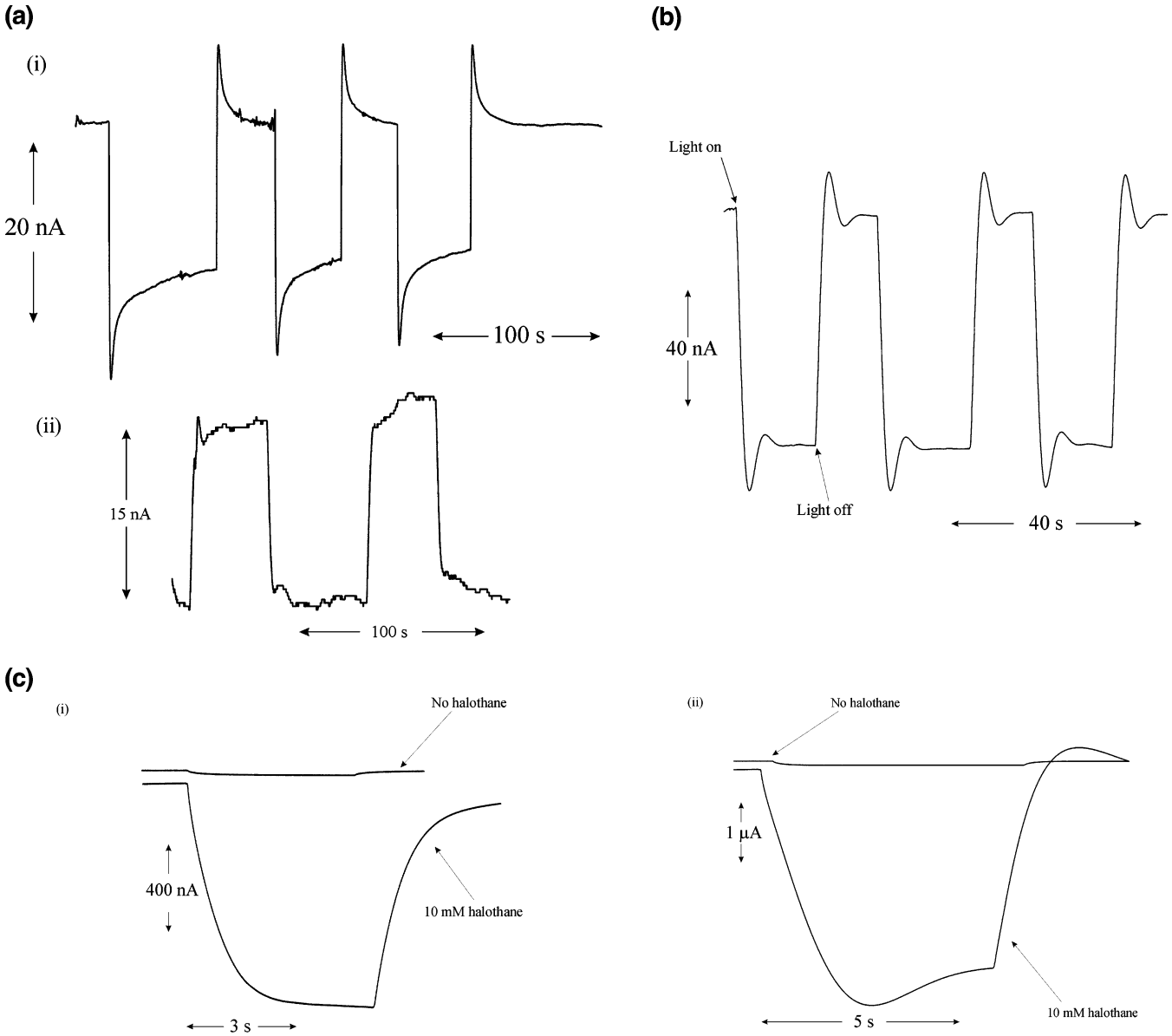

Figure 4. (a) Photocurrents observed for (i) the photoreduction at 0.0 V vs SCE and (ii) the photooxidation at 0.4 V vs SCE of 5 nmol of THPD deposited onto a 3×3 mm^2 bppg electrode immersed in 0.1 M $NaClO_4$ (2 mW cm^{-2}, 280 nm, solution flow rate 0.003 cm^3 s^{-1}). (b) Reductive photocurrents obtained for the conditions in (a, i) above, only with 10 mM halothane added into the aqueous solution and with irradiation at a wavelength of 320 nm. (c) Well-resolved phototransients (2 mW cm^{-2} illumination at 320 nm) observed for 5.4 nmol of THPD deposited on the 3×3 mm^2 bppg electrode potentiostated at 0.0 V vs SCE, immersed 0.1 M $NaClO_4$ containing 10 mM halothane (solution flow rate 0.003 cm^3 s^{-1}). (i) and (ii) are results from different experiments (see text).

$$\mathrm{THPD}(l) + \mathrm{h}\nu \rightleftharpoons \mathrm{THPD}^*(l) \quad \text{(E)}$$

$$\mathrm{THPD}^*(l) + \mathrm{CF_3CHClBr(aq)} \rightarrow \mathrm{THPD}^{+\bullet}(l) + \mathrm{CF_3CHClBr}^{-\bullet}(\mathrm{aq}) \quad \text{(F)}$$

$$\mathrm{CF_3CHClBr}^{-\bullet}(\mathrm{aq}) \rightarrow \mathrm{CF_3CHCl}^{\bullet}(\mathrm{aq}) + \mathrm{Br}^-(\mathrm{aq}) \quad \text{(G)}$$

Similar results were obtained for the cases of *tert*-butyl bromide and *tert*-butyl chloride instead of halothane in the aqueous phase and for all TRPD and DEDRPD oils studied. In this above scheme, as charge transfer arises from the activated form of the neutral molecule, electron transfer may take place across the liquid−liquid interface or within the microdroplets, given the lipophilicity of halothane.[49] In the former case, the electron transfer may be limited by the interfacial charge transfer rate or as a result of diffusion control within the aqueous phase. Assuming this latter case, we may estimate the photocurrent by

$$i_{\mathrm{diff}} = FAj = \frac{FAD[\mathrm{halothane}]_{\mathrm{bulk}}}{\delta} \quad (13)$$

where j is the aqueous flux of halothane to the liquid−liquid interface, F is the Faraday constant, D is the diffusion coefficient of halothane within the aqueous solution (ca. 10^{-5} cm^2 s^{-1}), $[\mathrm{halothane}]_{\mathrm{bulk}}$ is the bulk solution concentration of halothane (typically ca. 10 mM), δ is the Nernst thickness (typically around 100 μm), and A is the geometric surface area of the microdrop-

(49) (a) Orzech, C. E.; Genmill, F. Q., Jr. *Anal. Prof. Drug Subs.* **1985**, *14*, 597. (b) Hansch; C.; Vittoria, A.; Silipo, C.; Jow, P. Y. C. *J. Med. Chem.* **1975**, *18*, 546. (c) Leo, A.; Hansch, C.; Elkins, D. *Chem. Rev.* **1971**, *71*, 525.

lets. We approximate this latter quantity as the electrode area. Hence, eq 13 predicts a diffusion-controlled photocurrent in the order of 100 μA. This is much *greater* than that observed experimentally (up to a few microamps for this concentration of halothane), suggesting that, as for ascorbate, *diffusion of halothane within the aqueous phase does not affect the rate of the electron transfer process*.

The rate of THPD* reaction with halothane must therefore be limited by charge transfer across the liquid−liquid interface or take place within the femtoliter redox oil deposits due to the partitioning of halothane between the two phases. Accordingly, a partition coefficient of halothane between the THPD and the aqueous phases was determined (see Appendix) as $[\text{halothane}]_{\text{THPD}}/[\text{halothane}]_{\text{aq}} \approx 67$. Hence, *the partitioning and diffusion of halothane within the microdroplets are significant*. This is further verified by plots of reductive photocurrent against halothane concentration in the aqueous solution; in the range $5 < [\text{halothane}]/\text{mM} < 20$, some plots were observed to be linear, and others, not so. The lack of reproducibility in the plots suggests that processes other than electron transfer occur within the microdroplets.

Figure 4c shows typical photoreductive transients observed when 5.4 nmol of THPD are deposited on a bppg electrode held at 0 V versus SCE and illuminated at 320 nm in the presence of 10 mM halothane in an aqueous 0.1 M sodium perchlorate solution. In both cases, it can be seen that steady-state currents are reached after ca. 3 s. However, in one case, the photocurrent increases monotonically to its steady-state value; in the other, the photocurrent peaks at a maximum value *before* the photocurrent reaches its steady-state value. In both cases, the transient arises as a result of charge migration to the triple-phase boundary as noted above; the presence of a "hump" in the phototransient shortly after the light is switched on is due to a large concentration of halothane present at the three-phase boundary, as a consequence of the dark liquid−liquid halothane partitioning. Immediately after illumination, charge transfer takes place *within* the microdroplets, to form significant amounts of $\text{THPD}^{+\bullet}$, the immediate discharge of which at the three-phase boundary gives rise to an increase in current. However, as the irradiation continues, the concentration of halothane present in the droplet at the three-phase boundary decreases, and $\text{THPD}^{+\bullet}$ migrates (probably via both electron hopping, if the anion concentration (bromide) is sufficiently high, and by physical diffusion of $\text{THPD}^{+\bullet}$, likely as an ion pair) toward the three-phase boundary from other parts of the microdroplet (wherever the photochemical electron-transfer process is possible), leading to a fall off in the photocurrent and, thus, a maximum in the phototransient response. From the data illustrated in Figure 4c(i) for THPD, we may calculate an estimate of the diffusion coefficient of the $\text{THPD}^{+\bullet}$ ion pair within the organic deposits (D), assuming that this occurs exclusively in the classical Einstein−Schmoluchowski sense and that the radius of the (assumed hemispherical and monodispersed) microdroplets (R_0) is 2 μm:[12]

$$D \approx \frac{(\pi R_0)^2}{2\theta} \qquad (14)$$

In the above, θ is the time taken for the transient to reach a steady-state value (ca. 3 s). Thus, $D = 6.6 \times 10^{-8}$ cm^2 s^{-1}. This value is in agreement with that predicted by the Wilke−Chang expression as illustrated in previous work[7b] but is 2 orders of magnitude *smaller* than those estimated by White and coworkers for nitrobenzene anion radicals in neat nitrobenzene.[50] This contrast may likely arise as a consequence of the greater size of the $\text{THPD}^{+\bullet}$ ion pair *cf.* the nitrobenzene anion radical. It should be noted that electron hopping[50d] within the THPD deposits will in fact augment the diffusion rate, as would Marangoni convective forces that may operate.[6,7b] The above estimate is thus, to a first approximation, a lower estimate of the *diffusion* coefficient *within* femtoliter droplets.

Conclusions

Electron transfer reactions at, or within, unsupported femtoliter droplet arrays have been explored using redox liquid modified electrodes immersed into aqueous electrolytes. Voltmmetric oxidation of the electroactive oil (DEDRPD or TRPD) deposits takes place at or near the base circumference of the organic droplet (the three-phase boundary), where the oil "sees" both the electrode and the aqueous solution. In the absence of other aqueous-based redox species, electroneutrality within the oil environment dictates that either anion transfer into the oil from the aqueous electrolyte or electrogenerated cation release from the oil phase to the aqueous phase proceeds. When the aqueous phase contains an electroactive species (such as ascorbate or halothane), the organic deposit (electroformed or otherwise) may oxidize the aqueous species in two ways. If the species is very hydrophilic and cannot penetrate into the oil environment (such as ascorbate ions), electrocatalysis occurs over the droplet surface; lipophilic redox species (such as halothane) partition into the femtoliter deposits, and the mediated oxidation takes place from within the femtoliter environment. Although the exact mechanism for charge propagation within these very small deposits is not known (it probably takes place via diffusion, electron hopping, migration, Marangoni convection, or some admixture thereof), the work reported in this paper hints at the possibility of using this ilk of modified electrode as femtoscale electrochemical reactors, with applications to the understanding of acoustic emulsification electrosynthetic processes[51] or in the study of biomimetic processes such as photosynthesis. It is this latter case that is the subject of a forthcoming paper.[52]

Acknowledgment. The authors are grateful for helpful discussions with Dr. Nathan S. Lawrence. Further gratitude is expressed to Dr. Adam Clarke, Warwick University, for running NMR spectra. J.D.W. thanks the EPSRC for financial support via a studentship.

Appendix

Determination of the Partition Coefficient of Halothane between THPD and Water. Halothane is a lipophilic

(50) (a) Malmsten, R. A.; White, H. S. *J. Electrochem. Soc.* **1986**, *133*, 1067. (b) Malmsten, R. A.; Smith, C. P.; White, H. S. *J. Electroanal. Chem.* **1986**, *215*, 223. (c) Morris, R. B.; Fischer, K. F.; White, H. S. *J. Phys. Chem.* **1988**, *92*, 5306. (d) Norton, J. D.; Anderson, S. A.; White, H. S. *J. Phys. Chem.* **1992**, *96*, 3. (e) Paulson, S. C.; Okerlund, N. D.; White, H. S. *Anal. Chem.* **1996**, *68*, 581.
(51) (a) Wadhawan, J. D.; Marken, F.; Compton, R. G. *Pure Appl. Chem.* **2001**, *75*, 1947. (b) Banks, C. E.; Klymenko, O. V.; Compton, R. G. *Phys. Chem. Chem. Phys.* **2003**, *5*, 1652. (c) Compton, R. G.; Hardcastle, J. L.; del Campo, F. J.; Wadhawan, J. D. In *Encyclopaedia of Electrochemistry*, volume 3; Bard, A. J., Stratmann, M., Unwin, P. R., Eds.; Wiley-VCH: Germany, 2003; Chapter 2.10, p 328.
(52) Wadhawan, J. D.; Wain, A. J.; Compton, R. G. *ChemPhysChem*, in press.

anaesthetic.[49,53a] Partition coefficients, defined as $P = [\text{halothane}]_{\text{organic}}/[\text{halothane}]_{\text{water}}$, have been reported in *n*-octanol−water,[49b] and in blood or water,[49a,53a] tissue,[53a] oil,[53a] and rubber.[53a] The use of *n*-octanol as a reference solvent for partititon coefficient measurements arose as a result of its similarity to oils.[49c,53b] The *P* value for halothane in that system is[49b] 200. In this section, the partition coefficient of halothane between a THPD phase and an aqueous phase is estimated, using the "shake-flask" method[53b] as a result of its simplicity and ease of operation and ^{1}H NMR spectroscopy as our means of determination. The apparatus employed consists of two chambers, one containing halothane, the other containing both water and THPD. These latter two liquids are immiscible.[1−12] Nitrogen was bubbled into the halothane phase at the rate of about 30 gas bubbles per min, so as to (i) "carry" the volatile anaesthetic into the second chamber and (ii) emulsify effectively the THPD and the aqueous phases. The system was then left at room temperature (20 ± 2 °C) until all the halothane had transferred into the second chamber, whence the nitrogen supply was turned off so as to allow the system to phase separate. A drop of the less dense THPD phase was then examined via ^{1}H NMR, using deuterated chloroform as the solvent. Neat THPD has four equivalent aromatic protons (at 6.7 ppm) and 52 alkyl protons.[1] In contrast, halothane, with its single proton, exhibits a quartet[53c] centered at 5.8 ppm. THPD taken from the emulsion shows an additional peak at 5.8 ppm, due to halothane partitioning into the THPD phase. Based on the ratio of the THPD and halothane lines at 6.7 and 5.8 ppm, respectively (accounting for the proton difference), the mole ratio of THPD:halothane can be estimated (within 10% error) to be 1.25:1. Hence, given the solubility[49] of halothane in water (25 mM), the density[12] of THPD (0.93 g cm^{-3}) and the relative molecular mass of THPD (444), the partition coefficient of halothane between THPD and water is

$$P = \frac{[\text{halothane}]_{\text{THPD}}}{[\text{halothane}]_{\text{aq}}} = \frac{0.93/(1.25 \times 444)}{25 \times 10^{-6}} = 67.0 \pm 7.5 \quad (15)$$

Supporting Information Available: Table of values illustrating the wideness of the peak oxidation waves and the peak-to-peak potential separation for all DEDRPD oils with anions; table of values of k_{eff} for DEDHePD dissolution from the liquid−liquid interface for Br^-, NO_3^-, OCN^-, SO_4^{2-}, and F^- anions; table of values indicating the maxima in the absorption UV/visible spectra of all TRPD and DEDRPD oils (and their corresponding perchlorate salts); cyclic voltammograms for the oxidation of DEDBPD and DEDHPD in 0.1 M aqueous sodium perchlorate solutions; cyclic voltammograms for the oxidation of DEDBPD, DEDHPD, and DEDHePD in potassium thiocyanate solutions; cyclic voltammograms for the oxidation of DEDBPD and DEDHPD in 0.1 M aqueous potassium fluoride solutions; cyclic voltammograms for the oxidation of DEDHePD in aqueous 0.1 M potassium nitrate solutions (at two scan rates). This material is available free of charge via the Internet at http://pubs.acs.org.

JA030315P

(53) (a) Saidman, L. J. *Clin. Anesth.* **1968**, *1*, 11. (b) Bouchard, G.; Carrupt, P.-A.; Testa, B.; Gobry, V.; Girault, H. H. *Chem. Eur. J.* **2002**, *8*, 3478. (c) Brown, J. M.; Chaloner, P. A. *Can. J. Chem.* **1977**, *55*, 3380.